A glycopeptide in complex with MHC class I uses the GalNAc residue as an anchor

Vasso Apostolopoulos*†, Elizabeth Yuriev‡, Paul A. Ramsland*, Jodie Halton*, Carla Osinski*, Wenjun Li*, Magdalena Plebanski*, Hans Paulsen§, and Ian F. C. McKenzie*

*The Austin Research Institute, Heidelberg VIC 3084, Australia; ‡Victorian College of Pharmacy, Monash University, Parkville VIC 3052, Australia; and §Institute for Organic Chemistry, University of Hamburg, 20146 Hamburg, Germany

Edited by Philippa Marrack, National Jewish Medical and Research Center, Denver, CO, and approved October 13, 2003 (received for review April 16, 2003)

Peptides bind MHC class I molecules by anchoring hydrophobic side chains into pockets in the peptide binding groove. Here, we report an immunogenic (*in vitro* and *in vivo*) MUC1 glycopeptide (MUC1–8-5GalNAc) bound to H-2K^b, fully crossreactive with the nonglycosylated variant. Molecular modeling showed that the central P5-Thr-GalNAc residue points into the C pocket and forms van der Waals and hydrogen bond interactions with the MHC class I. As predicted, GalNAc, a modified peptide carrying an additional anchor in the central C anchor pocket, increased the affinity by ≈100-fold compared with the native low-affinity peptide (MUC1–8). The findings demonstrate that glycopeptides associated with MHC class I molecules can use GalNAc to anchor the peptide in the groove and enable high-affinity binding.

Antigen-presenting cells, primarily dendritic cells (DC), take up and process antigens and present peptides on MHC molecules. MHC class I consists of α1, α2, and α3 heavy chains and is noncovalently associated with β_2-microglobulin (light chain). The side chains of peptides (anchor residues) fit into pockets that extend along the floor of the groove of the α-chain. Crystallographic studies of MHC class I–peptide complexes have demonstrated that the peptide-binding groove is subdivided into various pockets (A–F) (1–3). Based on peptide elution and pool sequencing studies, it was demonstrated that MHC molecules had specific preferences for hydrophobic amino acids at certain positions along the peptide (4–6). Crystallographic studies of murine and human MHC class I molecules have shown that the N and C termini of the peptides are fixed and anchored in the groove by conserved interactions with the peptide backbone. For H-2K^b, anchors are in positions P2, P5, and P8 for 8-mer peptides; P2 binds into the B pocket, P5 into the C pocket, and P8 into the F pocket. The preferred amino acid residues that bind in the central C pocket are Phe/Tyr and that bind in the F pocket are Leu/Met. Some peptides, which do not contain the respective canonical anchor motifs, can still be presented by MHC molecules and act as effective targets for cytotoxic T lymphocytes (CTL) (7–12).

Synthetic glycopeptides with *O*-β-*N*-acetylglucosamine (GlcNAc) substitution on serine residues are efficiently transported by transporter associated with antigen processing into the endoplasmic reticulum (13), and a glycopeptide bound to MHC class I elicited glycopeptide-specific CTL in mice. Glycopeptide-specific T cells are also generated after immunization of mice with a synthetic peptide conjugated to GlcNAc (14). A peptide derived from vesicular stomatitis virus nucleocapsid (VSV8) had P6 [the T cell antigen receptor (TCR) contact residue] linked to galabiose disaccharide (15). The peptide retained its affinity to H-2K^b and activated glycopeptide-specific T cells (the peptide did not recognize the native VSV8 peptide). In another study, immunization with MHC class I H-2K^b restricted glycopeptide RGY8–6H-Gal2-generated T cells, which specifically lysed cells presenting the glycopeptide and not the native peptide (15). The crystal structure of H-2K^b in complex with RGY8–6H-Gal2 (16) demonstrated that the glycan position, linker length, and carbohydrate sizes were important for recognition by T cells. In addition, the crystal structure of a synthetic *O*-GlcNAc-bearing peptide in complex with MHC class I H-2D^b was determined (17), and MHC class I H-2D^b glycopeptide-specific CTL could be generated in mice. In these studies, the single glycan was exposed and directly recognized by the TCR. In all of these studies, the sugar residue pointed toward the TCR, allowing the T cells to specifically recognize the sugar residue.

MUC1 is a tumor-associated antigen highly expressed on many adenocarcinomas (breast, colon, lung, kidney, ovary, etc). Immunization of mice with mannan-MUC1 generates CD8$^+$ CTL, which protect mice against a MUC1$^+$ tumor challenge (10–12, 18, 19). It was demonstrated that the 9-mer peptide SAPDTRPAP (MUC1–9) is presented by H-2K^b (12), but the shorter 8-mer peptide, MUC1–8 (SAPDTRPA), binds with higher affinity than MUC1–9 and 100-fold lower affinity than high-affinity peptides OVA8, VSV8, and SEV9 (20). We determined the crystal structure of MUC1–8 peptide in complex with H-2K^b at 1.6 Å (20). MUC1–8 does not contain either Phe/Tyr at P5 nor Leu/Met at P8 that are usually associated with high-affinity binding to H-2K^b (5, 20). Instead, MUC1–8 has small nonpolar Ala residues at P2 and P8 and a small polar Thr residue at P5. MUC1–8 bound with the same overall features as with high-affinity peptides; however, a large cavity at the side of the C pocket was noted, and there was high flexibility of the central P5-Thr residue. We now demonstrate that MUC1–8 peptide with GalNAc linked to P5-Thr (MUC1–8-5GalNAc) binds to H-2K^b with high affinity and generates T cells both *in vitro* and *in vivo*, which recognize both MUC1–8 and MUC1–8-5GalNAc peptides. Molecular modeling suggests that the central P5-Thr-GalNAc points into the C pocket and forms unique hydrogen bonds and nonpolar van der Waals interactions with amino acid residues in the MHC class I, thus increasing the affinity binding of the peptide.

Materials and Methods

Peptides. SAPDTRPA, MUC1 VNTR (MUC1–8), SIINFEKL, chicken ovalbumin$_{257–264}$ (OVA8), and RGYVYQGL, VSV NP$_{52–59}$ (VSV8), were synthesized by using an Applied Biosystems model 430A machine. The purity of the peptides (>95%) were determined by MS. The glycopeptide SAPD(T-GalNAc)RPA (MUC1–8-5GalNAc) was synthesized by using solid-phase synthesis on Wang resin via a fluorenylmethoxycarbonyl (Fmoc) technique (21). The amino acids were coupled as Fmoc-pentafluorophenylester. The saccharide containing acetylated building blocks Fmoc-Thr-GalNAc was coupled with 2-(1H-benzotriazole-1-yl)-1,1,3,3-tetramethyluronium tetrafluoroborate (22). The cleavage from the resin was achieved with aqueous trifluoroacetic acid (95%). The deacetylation of the saccharide part was conducted with catalytic among NaOH/methanol at pH 8.5. The purification was carried out by reversed-phase HPLC with water/acetonitrile. Struc-

This paper was submitted directly (Track II) to the PNAS office.

Abbreviations: CTL, cytotoxic T lymphocytes; DC, dendritic cells; GlcNAc, *N*-acetylglucosamine; VSV, vesicular stomatitis virus; TCR, T cell antigen receptor.

†To whom correspondence should be addressed. E-mail: v.apostolopoulos@ari.unimelb.edu.au.

tural elucidation was performed with NMR spectroscopy, and the molecular weight was determined by matrix-assisted laser desorption ionization. The molecular weight for MUC1–8-5GalNAc (1,017.07) was found to be 1,017.19, and the purity of the MUC1–8-5GalNAc peptides was found to be >95% pure.

Generation of *in Vitro*-Specific CTL. Generation of primary *in vitro* CTL was performed as described (23, 24) with a few modifications. Briefly, 5×10^6 naïve spleen cells from C57BL/6 mice were cultured in 24-well plates (2 ml) in αMEM supplemented with 0.5% autologous mouse serum. Keyhole limpet hemocyanin (5 μg/ml), 25 ng/ml IL-7, and 10 μg/ml MUC1–8-5GalNAc were added to the culture, and on day 3, 10 units/ml IL-2 was added. On day 7, cells were recovered from bulk cultures and "semicloned" at 5–15,000 cells per well in 96 U-bottom well plates with 100,000 autologous irradiated (2,000 rad) peptide prepulsed (10 μg/ml) cells. IL-2 at 10 units/ml was added 24 h later. Seven days later, wells were tested for specific T cell activity in standard chromium release assays using EL4 cells or EL4 cells pulsed with MUC1–8-5GalNAc. Limiting dilution analysis from semicloned cultures was determined by using a minimum of 30 replicates of at least three responder cell doses by culturing with 1×10^5 C57BL/6 irradiated stimulator spleen cells pulsed with MUC1–8-5GalNAc. Seven days later, each microculture was assayed for cytotoxicity by replacing 100 μl of culture medium with 100 μl of target cell suspension containing ^{51}Cr-labeled EL4 or EL4-MUC1–8-5GalNAc pulsed tumor target cells. Wells were regarded as containing cytotoxic activity if they yielded specific ^{51}Cr release at >15% specific lysis.

Generation of DC and Immunization of Mice. H-2K^b C57BL/6 female 6- to 8-week-old mice were used in the experiments. Bone marrow cells from C57BL/6 female mice were cultured at 10^6 cells per ml in tissue culture, supplemented with 1,000 units/ml granulocyte–macrophage colony-stimulating factor, 10 μg/ml IL-4, and 10% FCS. At day 6, cells were washed and resuspended in the same cultured media and peptides were loaded on DC for 1 h. Pulsed DCs were washed, and 50 μl of 5×10^5 cells was injected intradermally in mice in the hind footpads. Ten days later, mice were boosted. After 10–14 days, mouse splenocytes were isolated and assessed by ELISPOT.

ELISPOT Assay. To assess IFN-γ production by CD8$^+$ T cells to MUC1–8 or MUC1–8-5GalNAc epitope, splenocytes from immunized mice were used in IFN-γ ELISPOT assays. Freshly isolated spleen cells were incubated with titrating concentrations (10^{-6}–10^{-9} M) of MUC1–8, MUC1–8-5GalNAc, irrelevant peptide OVA8, ConA, or no peptide for 18 h at 37°C on nitrocellulose plates (precoated with an anti-murine IFN-γ mAb). Cells were washed from the plates, and plates were incubated with biotin-conjugated mAb to murine IFN-γ followed by a streptavidin-alkaline phosphatase (AP) conjugate. Spots of AP activity were detected by using colorimetric AP detection and counted on an ELISPOT reader. The data are presented as spot-forming units per 1×10^6 cells. Experiments were performed two to three times.

Molecular Modeling. Molecular modeling was carried out by using the HYPERCHEM modeling package (version 5.11). AMBER force field was used for molecular mechanics geometry optimization. The molecular structures were optimized by using the conjugate gradient algorithm (Polak-Ribiere) *in vacuo* with the termination condition being rms gradient <0.1 kcal/(molχÅ). Aqueous solvent conditions were simulated with the distance-dependent dielectric. No cutoffs were used, and scale factors of 0.5 were set for 1,4-nonbonded interactions.

Molecular dynamics simulations were carried out for MUC1–8 and MUC1–8-5GalNAc peptides in the context of the binding groove of the α-domain of the H-2K^b molecule. The coordinates (Protein Data Bank ID code 1G7Q) for the crystal structure of MUC1–8 in complex with H-2K^b were used. The peptide molecules were heated to room temperature (300 K) for 100 ps and then simulated at room temperature for an additional 500 ps. The time step was 0.001 ps, and the temperature step was 30 K/ps.

Affinity Measurements of Peptides Bound to H-2K^b. Affinity measurements for binding of peptides to soluble K^b molecules were performed as described (25, 26). Briefly, VSV8 peptide was labeled with ^{125}I by using the Iodogen method. The ^{125}I-VSV8 peptide was purified by using a Sep-Pak column (Waters). The specific activity of the peptide was assessed as cpm/ng. The competition assays were performed at 4°C, 23°C, and 37°C as described (20, 25–27) with a few modifications. The binding studies were carried out in 1% FCS, and the free peptide was removed by gel filtration on Sephadex columns (NAP-5, Pharmacia Biotech). The dissociation constants for unlabeled peptides were determined from the molar concentrations of unlabeled peptides that gave 50% inhibition of ^{125}I-VSV8 binding to K^b molecules. All affinity measurements were done in parallel, and the values are a mean of three to five values.

Peptide Stabilization Using RMA-S Cells. MHC class I molecules in the murine cell line RMA-S (C57BL/6 transporter associated with antigen processing-deficient cells) can be used to measure the direct binding of peptides to class I molecules. RMA-S cells were incubated with (10^{-6} to 10^{-10} M), MUC1–8, MUC1–8-5GalNAc, or high-affinity control peptide OVA8 at 26°C for 3 h and used in flow cytometry. Anti-H-2K^b (HB-158) IgG2a as supernatant (100 μl) was added to 2×10^5 RMA-S peptide-loaded cells and incubated for 45 min at 4°C. After washing with 0.5 ml of phosphate buffer, 100 μl of 1:50 dilution of FITC-conjugated sheep (Fab′)$_2$ anti-mouse Ig was added and incubated for 45 min at 4°C; after further washing, the cells were analyzed by FACScan.

Results

Generation of *in Vitro*-Primed CTL. To detect CTL activity, cloning on day 7 after the initial bulk stimulation was performed by using high effectors at 5–15,000 cells per well. Seven days after semicloning, wells were tested for specific CTL activity in CTL assays using EL4 cells or EL4-MUC1–8-5GalNAc pulsed target cells. It can be seen that CTL from 18/30 wells (60%) specifically lysed EL4-MUC1–8-5GalNAc targets; EL4 cells were not lysed (Fig. 1*A*). Limiting dilution analysis from *in vitro*-primed T cells indicated that the precursor frequency of the specific T cells to MUC1–8-5GalNAc to be 1/13,600 (Fig. 1*B*). In comparison, the precursor frequency of MUC1–8 *in vitro*-primed T cells was 1/28,000, indicating more efficient clonal T cell priming by the MUC1–8-5GalNAc as compared with MUC1–8 peptide. In addition, limiting dilution analysis from *in vitro*-primed T cells to MUC1–8-5F8L (a MUC1–8 peptide mutated at the anchor sites, to increase the affinity) (20) indicated a precursor frequency of 1/15,000 (data not shown), indicating that the T cells that were generated against the mutated higher affinity binding peptide recognized the mutated peptide more efficiently compared with the nonmuatated peptide. All of the *in vitro* T cells were generated by using the same culture conditions and in parallel. The precursor frequency of MUC1–8-5GalNAc peptide *in vitro*-generated T cells was 2-fold higher than MUC1–8 peptide-generated T cells. A 2-fold increase in precursor frequency can have dramatic effects on protective efficacy of peptides *in vivo*. We have demonstrated this for a range of MUC1 antigen formulations, where the precursor frequency correlated with tumor protection, and even a 2-fold increase gave dramatic effects (28). In addition, ours and other studies in liver-stage malaria have shown a 4-fold increase in protective efficacy of CD8 T cells upon a 2-fold increase in precursor frequency (from 1/8,000 to 1/4,000) (23). Importantly, the difference in these frequency values is statistically significant, indicating MUC1–8-5GalNAc binds with higher affinity, providing quantitative functional data to corroborate the binding assay data (see below). We have been able to generate specific CTL *in vitro* to

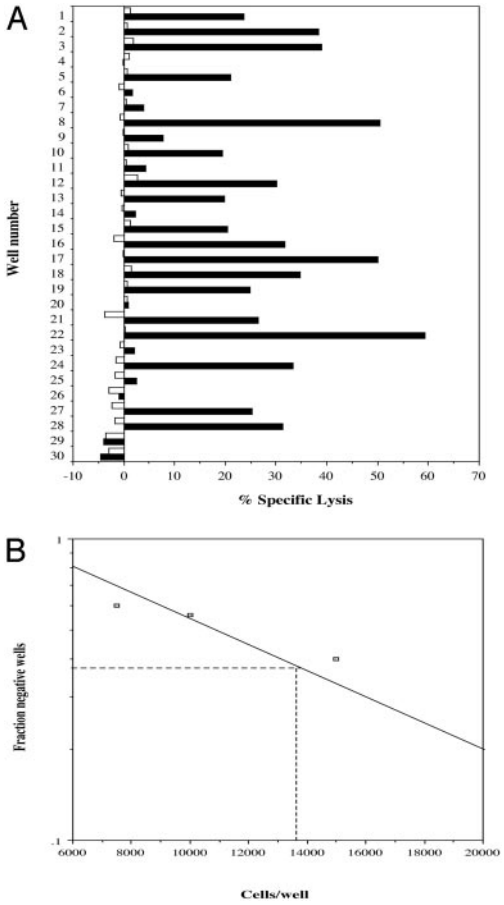

Fig. 1. *In vitro*-primed CTL and precursor frequency determination. (*A*) CTL activity of semicloned T cells. Naïve T cells prepulsed with 10 μg/ml MUC1–8-5GalNAC peptide were cultured for 7 days in bulk culture in the presence of IL-2/IL-7/keyhole limpet hemocyanin. Cells were semicloned. Cells from individual wells were tested for specific CTL activity after 7 days of culture. The effector-to-target cell ratio was calculated to average 5:1 for the semicloning. EL4 (open bars) or EL4-MUC1–8-5GalNAc pulsed targets (10 μg/ml) (filled bars) were chromium-labeled. Data are shown as percentage of specific lysis as described (23, 24). (*B*) Precursor frequencies of semicloned T cells specific for MUC1–8-5GalNAc peptide were determined as the inverse of responder cell dose required to generate 37% negative wells.

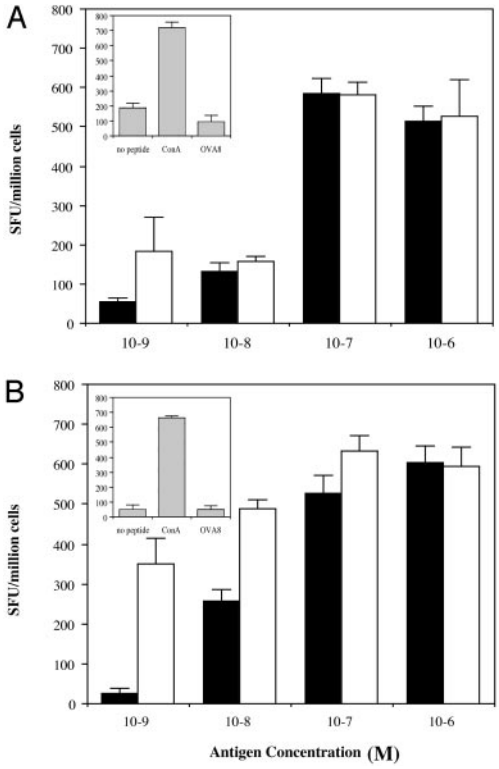

Fig. 2. Measurement of IFN-γ secreted by T cells as measured by ELISPOT assay. Mice were immunized with DC-MUC1–8 (*A*) or DC-MUC1–8-5GalNAc (*B*). In both immunized mouse groups, specific IFN-γ-secreting T cells are generated that recognize both MUC1–8 (filled columns) and MUC1–8-5GalNAc (empty columns) peptides. OVA8 was used as a negative control, and ConA was used as a positive control.

MUC1–8-5GalNAc at a high frequency, comparable to a high-affinity peptide. Although we have not formally demonstrated clonality in our study, in similar assays of limiting dilution of primary cultures, at the limiting dilution end of <1 positive cell per 30 wells, cells are clonal (23, 24).

Generation of T Cells *in Vivo*. The ability of MUC1–8 or MUC1–8-5GalNAc to induce T cells responses was measured by using IFN-γ in ELISPOT analysis after recognition of 10^{-6} to 10^{-9} M MUC1–8 or MUC1–8-5GalNAc peptides. Mice immunized with DC-MUC1–8 generated IFN-γ-secreting T cells that recognized MUC1–8 and MUC1–8-5GalNAc peptides similarly at 10^{-6}, 10^{-7}, and 10^{-8} M; however, at 10^{-9} M concentration of the peptides MUC1–8-5GalNAc was recognized more efficiently (suggesting that MUC1–8-5GalNAc binds with higher affinity) (Fig. 2*A*). Likewise, mice immunized with MUC1–8-5GalNAc (Fig. 2*B*) T cells recognized both MUC1–8 and MUC1–8-5GalNAc; however, MUC1–8-5GalNAc being of higher affinity was recognized more efficiently. Nonimmunized mice did not recognize either MUC1–8 or MUC1–8-5GalNAc peptides (data not shown). Thus, T cells are able to recognize both MUC1–8 and MUC1–8-5GalNAc. This finding was surprising, as all glycopeptides identified to date, presented by either MHC class I or MHC class II generate specific T cells that do not recognize the native nonglycosylated peptide. These results suggested that the Thr-GalNAc residue may be pointing into the peptide binding groove. To gain insights into the binding of MUC1–8-5GalNAc with H-2K^b, we modeled MUC1–8-5GalNAc peptide with H-2K^b using the crystal structure of MUC1–8-H-2K^b complex as a template.

Binding of MUC1–8-5GalNAc Peptide with H-2K^b. Molecular dynamics simulation run for the MUC1–8 peptide revealed that, as predicted (20), the Thr exhibits a high degree of side-chain motion within the central C pocket. When the Thr torsion angle t ($C_{C=O}$-Cα-Cβ-Cγ) was monitored during the molecular dynamics run, it displayed preference for several regions. Significantly preferred are ranges $\approx\pm180°$ (characteristic of the conformation in the crystal structure, ref. 20) and 60°. Conformations with the torsion t displaying values around 0° are also observed, although to a much lesser extent. When the Thr residue was modified by attaching the GalNAc moiety and the peptide was subjected to further room temperature simulation, the preference for the 60° range became almost absolute with the 180° range becoming completely inaccessible and the 0° range observed only for 10 ps. The two peptide structures (MUC1–8 and MUC1–8-5GalNAc) were analyzed in terms of space complementarity, GalNAc moiety position in the groove, and the intermolecular interactions. For the MUC1–8-5GalNAc peptide, the structure observed at 300 ps in the molecular dynamics run ($t = 53°$) was used. Compared with MUC1–8, the complex containing MUC1–8-5GalNAc buries additional 21 Å^2 of the surface area (12 Å^2 for peptide and 9 Å^2 for protein). Although these values are relatively small, the visualization of the solvent-accessible surfaces in the two

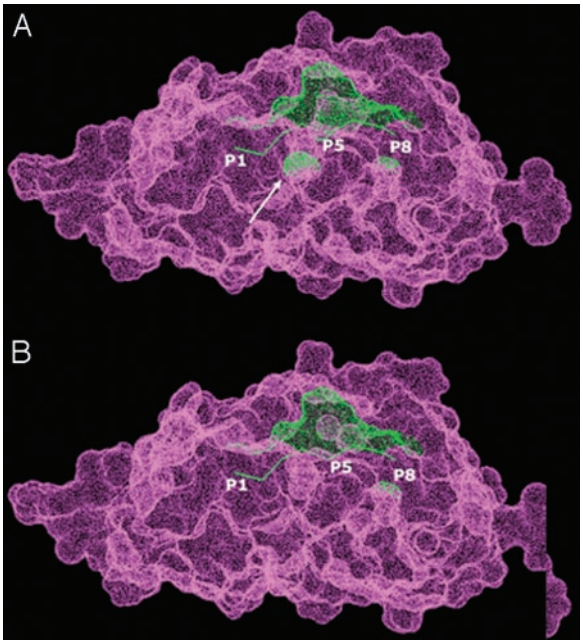

Fig. 3. Solvent-accessible surfaces. Shown are MUC1–8 (*A*) and MUC1–8-5GalNAc (*B*) in complex with H-2K^b. The complex with MUC1–8 has an internal cavity in the C pocket (shown by the white arrow) and, as previously demonstrated, of the crystal structure of MUC1–8 in complex with H-2K^b (20). When the surface representation is generated for the complex with MUC1–8-5GalNAc peptide (*B*), it is clear that this cavity no longer exists. Peptide residues P1, P5, and P8 are labeled. Surfaces of the peptide residues that are contributed to by the residues of the protein (α-domain, pink) and the peptide (green) are shown. The figure was drawn with INSIGHT II.

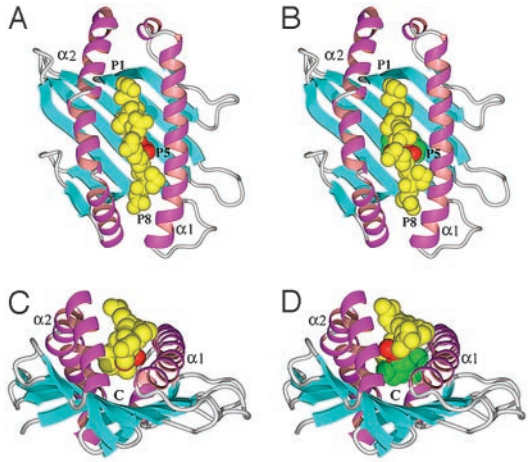

Fig. 4. Space-filling representation of peptides in complex with MHC class I. MUC1–8 (*A* and *C*) and MUC1–8-5GalNAc (*B* and *D*). *A* and *B* are viewed from above the MHC class I, and *C* and *D* are viewed from the side. The α-domains of the MHC are shown in pink and the β-sheet floor in cyan. The position of the C pocket is indicated, and the important C pocket residues, Val-9, Tyr-22, Asn-70, Ser-73, Phe-74, Val-97, Ser-99, Gln-114, and Tyr-116, are omitted for clarity. Peptides are shown in Corey Pauling Kultun representations (yellow), the central P5 Thr is in red, and the GalNAc group is in green. The figure was drawn with INSIGHT II.

complexes highlights the significance of the differences. Specifically, in the complex with the MUC1–8 peptide (Fig. 3*A*) the internal cavity could be observed (as indicated by the white arrow), the surface of which contributed to the residues of the protein (α-domain, pink) and the peptide (green). When the surface representation is generated for the complex with MUC1–8-5GalNAc peptide (Fig. 3*B*), it is clear that this cavity no longer exists. This finding demonstrates a better shape complementarity between the two components of the complex.

The above observations are confirmed by comparison of the relative occupancy or space filling of the H-2K^b C-specificity pocket, by MUC1–8 and MUC1–8-5GalNAc (Fig. 4). The P5-Thr residue in MUC1–8 only partially compensates in filling the C pocket space, whereas the P5-Thr-GalNAc in MUC1–8-5GalNAc points down into the peptide binding C pocket, filling the cavity. Superposition of the H-2K^b $\alpha1/\alpha2$ domain of MUC1–8 and MUC1–8-5GalNAc show similar overlays and angle values when viewed from the side (Fig. 5*A*). Strikingly, P5 Thr-GalNAc residue in MUC1–8-5GalNAc overlays in the same direction as P5 Thr in MUC1–8, with the GalNAc residue occupying the binding pocket. Furthermore, superposition of MUC1–8-5GalNAc with high-affinity canonical anchor-containing peptides, OVA8 and VSV8, shows similar overlays (Fig. 5*B*). Of particular interest, the P5 Thr-GalNAc residue in MUC1–8-5GalNAc occupies the same amount of space and is overlaid with Phe/Tyr in OVA8/VSV8, respectively, into the C pocket. These data indicate that the P5 Thr-GalNAc residue in MUC1–8-5GalNAc points into the C pocket and may act as an anchor residue.

Interactions of MUC1–8-GalNAc Peptide with H-2K^b. Analysis of the complexes of H-2K^b with peptides MUC1–8 and MUC1–8-5GalNAc demonstrates increased intermolecular interactions exhibited by P5 Thr-GalNAc as compared with P5 Thr residue (Fig. 5*C*). Whereas in the MUC1–8 peptide, the P5 Thr residue demonstrates several hydrogen bonds to the surrounding protein residues, in the MUC1–8-5GalNAc peptide the intermolecular interactions are augmented by nonpolar van der Waals contacts of GalNAc to the Phe-74 protein residue ($\alpha1$-domain) (Fig. 5*C*). In addition, the P5 Thr in MUC1–8 forms hydrogen bonds only with Ser-73 and Asn-70 from the $\alpha1$-domain of the MHC, whereas P5 Thr-GalNAc forms hydrogen bonds not only with Ser-73 and Asn-70 but also with Ser-99, which is buried on the β-sheet floor within the C pocket (Fig. 5*C*). Furthermore, P5 Thr-GalNAc residue makes additional contacts with Val-9, Tyr-22, Val-97, Gln-114, and Tyr-116, which are in the peptide binding pocket, C. The increase in the number of interactions of P5 Thr-GalNAc with H-2K^b as compared with the number of interactions of P5 Thr suggests a higher affinity of MUC1–8-5GalNAc peptide to H-2K^b compared with the native nonglycosylated peptide, MUC1–8. Thus, we determined the affinity of MUC1–8-5GalNAc to soluble H-2K^b and its ability to stabilize H-2K^b in RMA-S cells.

Affinity Measurements of MUC1–8-5GalNAc with H-2K^b. We measured the affinity of MUC1–8-5GalNAc in the same inhibition assay as used for MUC1–8 (20) and found it to be 1.3×10^{-8} M at 23°C and 3.8×10^{-7} M at 37°C, similar in magnitude to that of high-affinity OVA8, VSV8, or MUC1–8-5F8L peptides (Table 1) (20). The addition of GalNAc to Thr-P5 clearly increased the affinity by ≈60-fold at 23°C and 100-fold at 37°C when compared with MUC1–8 peptide. Hence, this finding confirmed the prediction that GalNAc provides additional stabilizing interactions to the original MUC1–8 H-2K^b complex.

Stabilization of MHC Class I on RMA-S Cells with MUC1–8-5GalNAc. To confirm the above molecular binding studies in a model peptide-MHC binding in live cells, we examined the binding of MUC1–8, MUC1–8-5GalNAc, and OVA8 peptides to H-2K^b in assembly assays, based on peptide-dependent stabilization of MHC heavy chains in transporter associated with antigen processing-deficient cells (RMA-S). MUC1–8 stabilized MHC class I, H-2K^b, at 10^{-6} to 10^{-7} M; conversely, MUC1–8-5GalNAC stabilized H-2K^b, at 10^{-6} to 10^{-9} M; high-affinity peptide OVA8 stabilized H-2K^b strongly at 10^{-6} to 10^{-9} M and very weakly at

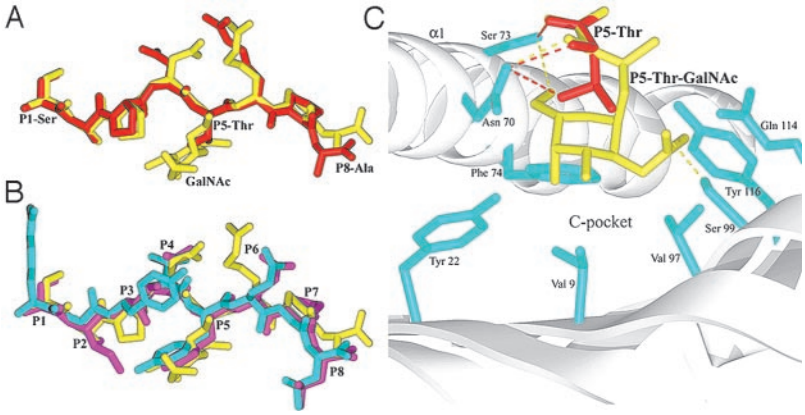

Fig. 5. Structure comparisons of selected H-2K^b-bound peptides. (*A*) Comparison of MUC1–8 and MUC1–8-5GalNAc peptides viewed from the side. (*B*) OVA8 and VSV8 are superimposed with MUC1–8-5GalNAc and viewed from the side. The peptide conformations represent their structures in the H-2K^b bound form. Peptide colors are: MUC1–8, red; MUC1–8-5GalNAc, yellow; OVA8, cyan; VSV8, magenta. (*C*) Interactions of P5 residue Thr (MUC1–8, red) and Thr-GalNAc (MUC1–8-5GalNAc, yellow) to MHC (cyan) and within the C specificity pocket. H-bond interactions are shown. The GalNAc residue in MUC1–8-5GalNAc makes additional interactions with all of the residues shown, which are not present in the MUC1–8 peptide. The figure was drawn with INSIGHT II.

10^{-10} M (Fig. 6). Thus, MUC1–8-5GalNac was able to stabilize H-2K^b molecules on RMA-S cells ≈100-fold more efficiently than MUC1–8 and marginally less efficiently than OVA8 (Fig. 6). The affinity measurements were similar in magnitude when testing the binding of these peptides to soluble H-2K^b *in vitro* and in live cells (Table 1 and Fig. 6), suggesting use of the C pocket by GalNac can occur by exogenous addition to MHC and during natural peptide–MHC complex assembly.

Discussion

Glycosylation of T cell epitopes has been repeatedly reported to abolish their ability to be recognized by T cells specific for their nonglycosylated form. Here, we show that a glycosylated epitope can be fully crossreactive. This unusual crossreactivity could be explained by the binding of the GalNAc residue into the C pocket of MHC class I, providing not only an equivalent surface for TCR recognition, but higher affinity binding to the glycosylated compared with the nonglycosylated epitope. The use of carbohydrate residues as anchors provides a modality for T cell epitope binding to the MHC molecule.

Recognition of peptide-MHC by T cells initiates a cascade of signals in T cells, which maintains a T cell-dependent immune response. An understanding of how peptides bind to MHC class I molecules is important for determination of the physiology of immune responses and manipulation of peptides to affect immune responses. Thus far, the crystal structures of high-affinity binding peptides to MHC have been determined. High-affinity peptides bind to MHC class I molecules with preferred amino acids at certain positions within pockets of the peptide binding groove. The mode of binding of high-affinity peptides (VSV8, OVA8, and SEV9) to murine MHC class I H-2K^b has been demonstrated by crystal structures (2, 3). We recently determined the crystal structure of an antigenic MUC1 peptide, MUC1–8, which lacked canonical anchors and bound with low affinity (20). MUC1–8 bound similarly to the high-affinity peptides; however, the central C pocket was virtually empty, leaving a large cavity, where small P5 Thr bound (20). We also demonstrated that a high-affinity peptide, derived from yeast (SRDHSRTPM), bound with high affinity, which did not contain the canonical Phe/Tyr residue (27); this peptide made use of an alternative pocket, the E pocket.

Table 1. Affinity measurements of peptides binding to H-2K^b

Peptide	Sequence	23°C K_D, nM	37°C K_D, nM
MUC1–8	SAPDTRPA	877	37,000
MUC1–8-5F8L	SAPDFRPL	60	300
MUC1–8-5GalNAc	SAPDT **(Ga1NAc)** RPA	13	380
OVA8	SIINFEKL	10	82
VSV8	RGYVYQGL	27	163

Mucins, and other O-linked glycoconjugates, which are found in the cytoplasm and nucleus, contain monosaccharide or disaccharides attached to serine, threonine, or tyrosine residues (29, 30). It was recently demonstrated that DC are able to endocytose, process, and present to MHC class II a MUC1 100-mer glycopeptide comprising GalNAc residues (which includes the sequence of MUC1–8-5GalNAc) without removal of the GalNAc residues (31). Herein, we demonstrate a MUC1 glycopeptide that generates CD8$^+$ T cells. A number of studies have demonstrated that a variety of glycopeptides are presented to MHC molecules. The mouse hemoglobin-derived peptide$_{67–76}$ binds to I-E^k, and T cells are generated that recognize the GalNAc residue (32, 33). T cells

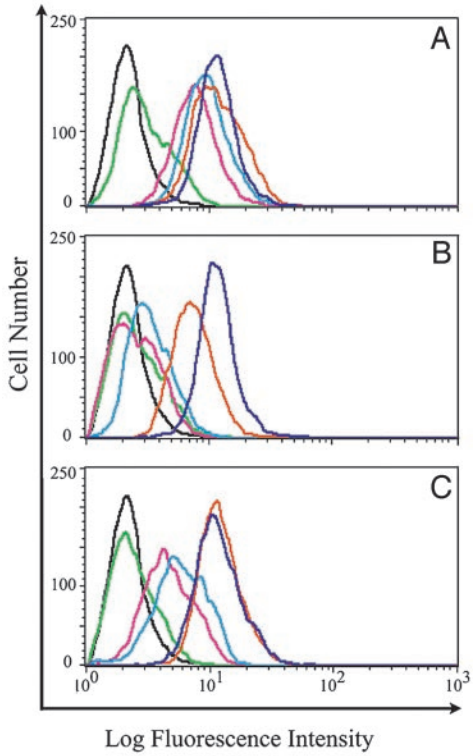

Fig. 6. Stabilization of MHC class I molecules by MUC1–8, MUC1–8-5GalNAc, and OVA8 peptides. Flow cytometric analysis of RMA-S cells pulsed with OVA8-positive control high-affinity peptide binder (*A*), native peptide MUC1–8 (*B*), and glycopeptide MUC1–8-5GalNAc (*C*), before incubation with anti-H-2K^b-specific antibody. Titrating peptide concentrations were added and labeled as 10^{-6} M (dark blue), 10^{-7} M (orange), 10^{-8} M (light blue), 10^{-9} M (pink), 10^{-10} M (green), and no peptide (black).

IMMUNOLOGY

against a type II collagen$_{256–270}$ glycopeptide from rheumatoid arthritis were identified (34, 35). Other carbohydrate-specific T cells have been identified against bee venom allergen phospholipase A2 (36) and to hen egg lysozyme$_{52–61}$ (37, 38). In these studies T cells specifically recognized the glycopeptide.

The H-2K^b peptide, VSV8, with galabiose disaccharide attached to the P6 residue has been shown to activate carbohydrate-specific T cells (15), and the crystal structure of H-2K^b-VSV8 glycopeptide demonstrated that the P6-glabiose residue pointed toward the TCR (16). A synthetic O-GlcNAc peptide from Sendai virus nucleoprotein (SEV9) in complex with MHC class I H-2D^b (K2G) is able to induce glycan-specific CTL (14) in mice. The crystal structure demonstrated that the O-GlcNAc residue pointed away from the peptide binding groove and toward the TCR (17). Furthermore, glycosylated peptides (with GlcNAc pointing toward the TCR) have been identified to be presented by MHC class I *in vivo*, after their isolation from HLA-A2+ cells, using wheat germ agglutinin lectin affinity chromatography (39).

Herein, we demonstrate that glycosylation of the central peptide residue (P5 Thr in MUC1–8) places the carbohydrate within the central C pocket and yields CTL that recognize both MUC1–8 and MUC1–8-5GalNAc peptides. MUC1–8 incorporating a disaccharide (GalGalNAc) did not induce CTL *in vitro* or *in vivo* and failed to bind to H-2K^b molecules (data not shown). In contrast, GalNAc monosaccharide (MUC1–8-5GalNAc) generated T cells both *in vitro* and *in vivo*. The MUC1–8-5GalNAc-specific T cells were not able to discriminate between the glycosylated (MUC1–8-5GalNAc) or native (MUC1–8) peptides. Similarly, MUC1–8-specific T cells were also not able to discriminate between the glycosylated and native peptides. This finding indicates that the central Thr-GalNAc residue does not point toward the TCR but down into the binding pocket. The specificity between the monosaccharide (GalNAc) compared with the disaccharide (GalGalNAc) suggests that the cavity in the native peptide can be accommodated only by a short monosaccharide linker, GalNAc. Further, GalGalNAc attached to the Thr residue prevented binding of the peptide to soluble MHC H-2K^b and was not able to stabilize RMA-S cells, indicating GalNAc residue is pointing down into the pocket, because the longer GalGalNAc residue abolished its ability to bind to H-2K^b. If the GalNAc residue was pointing toward the TCR, then the longer GalGalNAc-containing peptide, would also bind to H-2K^b. In addition, molecular modeling of MUC1–8-5GalNAc in complex with H-2K^b (based on the crystal structure of MUC1–8) demonstrated that the internal cavity within the central binding C pocket present in MUC1–8 was no longer present in MUC1–8-5GalNAc. This finding further indicates that GalNAc residue uses the central C pocket to anchor the peptide. We have performed binding (binding to soluble H-2K^b molecules or by stabilization of RMA-S cells) of the following MUC1–8 mutated peptides: SAPDTRPA to SAPDFRPA; SAPDTRPA to SAPDYRPA; SAPDTRPA to SAPDFRPL; SAPDTRPA to SAPDYRPL. All mutated peptides demonstrated higher affinity binding to H-2K^b and better stabilization of RMA-S cells. Similar findings have been demonstrated by others (40, 41). Interestingly, superposition of P5 Thr-GalNAc with high-affinity, canonical anchor motif peptides, OVA8 and VSV8, which use P5 Phe/Tyr in the C pocket, respectively, to anchor the peptide, are similarly overlaid. Analysis of the interaction in the modeled complexes (MUC1–8 compared with MUC1–8-5GalNAc) demonstrates that P5 Thr-GalNAc makes additional intermolecular interactions (van der Waals contacts and hydrogen bonds) with MHC residues as compared with P5 Thr. These interactions suggest an increase in affinity binding of MUC1–8-5GalNAc to H-2K^b compared with MUC1–8 binding. Affinity measurements and stabilization of H-2K^b on RMA-S cells confirmed the modeling. The increase in affinity of MUC1–8-5GalNAc peptide to soluble H-2K^b and the increase in the ability to stabilize RMA-S transporter associated with antigen processing-deficient cells as compared with the native (MUC1–8) peptide further indicates that the MUC1–8-5GalNAc peptide uses the GalNAc residue to anchor the peptide to MHC class I, H-2K^b.

The molecular interactions elucidated in glycopeptide-MHC complexes and the use of the GalNAc residue to increase the affinity of peptide binding should help define additional immunogenic peptides from primary protein sequences and aid in the design of alternative approaches for vaccines.

This work was supported by National Health and Medical Research Council Project Grant 223310 (to V.A.) and The Austin Research Institute (V.A., P.A.R., M.P., and I.F.C.M.). V.A. is a National Health and Medical Research Council R. Douglas Wright Fellow (223316), and M.P. is a Howard Hughes Scholar and National Health and Medical Research Council Senior Fellow.

1. Garrett, T. P. J., Saper, M. A., Bjorkman, P. J., Strominger, J. L. & Wiley, D. C. (1989) *Nature* **342,** 692–696.
2. Fremont, D. H., Matsumura, M., Stura, E., Peterson, P. A. & Wilson, I. A. (1992) *Science* **257,** 919–927.
3. Fremont, D. H., Stura, E., Matsumura, M., Peterson, P. A. & Wilson, I. A. (1995) *Proc. Natl. Acad. Sci. USA* **92,** 2479–2483.
4. Falk, K., Rotzschke, O., Stevanovic, S., Jung, G. & Rammensee, H. G. (1991) *Nature* **351,** 290–296.
5. Rammensee, H. G., Friede, T. & Stevanovic, S. (1995) *Immunogenetics* **41,** 178–228.
6. Rammensee, H. G. (1995) *Curr. Opin. Immunol.* **7,** 85–96.
7. Daser, A., Urlaub, H. & Henklein, P. (1994) *Mol. Immunol.* **31,** 331–336.
8. Mandelboim, O., Bar-Haim, E., Vadai, E., Fridkin, M. & Eisenbach, L. (1997) *J. Immunol.* **159,** 6030–6036.
9. Gao, L., Walter, J., Travers, P., Stauss, P. & Chain, B. (1995) *J. Immunol.* **155,** 5519–5526.
10. Apostolopoulos, V., Haurum, J. & McKenzie, I. (1997) *Eur. J. Immunol.* **27,** 2579–2587.
11. Apostolopoulos, V., Karanikas, K., Haurum, J. & McKenzie, I. (1997) *J. Immunol.* **159,** 5211–5218.
12. Apostolopoulos, V., Chelvanayagam, G., Xing, P. X. & McKenzie, I. F. C. (1998) *J. Immunol.* **161,** 767–775.
13. Haurum, J. S., Hoier, I. B., Arsequell, G., Neisig, G., Valencia, G., Zeuthen, Z., Neefjes, J. & Elliott, T. (1999) *J. Exp. Med.* **190,** 145–150.
14. Haurum, J. S., Arsequell, G., Lellouch, A. C., Wong, S. Y., Dwek, R. A., McMichael, A. J. & Elliot, T. (1994) *J. Exp. Med.* **180,** 739–744.
15. Abdel-Motal, U. M., Berg, L., Rosen, A., Bengtsson, M., Thorpe, C. J., Kihlberg, J., Dahmen, J., Magnusson, G., Karlsson, K. A. & Jondal, M. (1996) *Eur. J. Immunol.* **26,** 544–551.
16. Speir, J. A., Abdel-Motal, U. M., Jondal, M. & Wilson, I. A. (1999) *Immunity* **10,** 51–61.
17. Glithero, A., Tormo, J., Haurum, J. S., Arsequell, G., Valencia, G., Edwards, J., Springer, S., Townsend, A., Pao, Y. L., Wormald, M., *et al.* (1999) *Immunity* **10,** 63–74.
18. Apostolopoulos, V., Pietersz, G. A., Loveland, B., Sandrin, M. & McKenzie, I. (1995) *Proc. Natl. Acad. Sci. USA* **92,** 10128–10132.
19. Apostolopoulos, V., Pietersz, G. A. & McKenzie, I. (1996) *Vaccine* **14,** 930–938.
20. Apostolopoulos, V., Yu, M., Corper, A. L., Teyton, L., Pietersz, G. A., Plebanski, M., McKenzie, I. & Wilson, I. A. (2002) *J. Mol. Biol.* **318,** 1293–1305.
21. Peters, S., Bielfeld, M., Meldal, K., Bock, H. & Paulsen, H. (1992) *J. Chem. Soc. Perkin Trans.* 1163–1171.
22. Mathieux, N., Paulsen, H. & Meldal, K. (1997) *J. Chem. Soc. Perkin Trans.* 2358–2368.
23. Plebanski, M., Allsopp, C., Aidoo, M., Reyburn, H. & Hill, A. (1994) *Eur. J. Immunol.* **25,** 1783–1787.
24. Plebanski, M., Lee, E. A. M., Hannan, C. M., Flanagan, K. L., Gilbert, S. C. & Hill, A. (1999) *Nat. Med.* **5,** 565–571.
25. Matsumura, M., Saito, Y., Jackson, M., Song, E. & Peterson, P. A. (1992) *J. Biol. Chem.* **267,** 23589–23595.
26. Stura, E. A., Matsumura, M., Fremont, D., Saito, Y., Peterson, P. & Wilson, I. A. (1992) *J. Mol. Biol.* **228,** 975–982.
27. Apostolopoulos, V., Yu, M., Corper, A. L., Li, W., Plebanski, M., McKenzie, I. F. C., Teyton, L. & Wilson, I. A. (2002) *J. Mol. Biol.* **318,** 1307–1316.
28. Pietersz, G. A., Li, W., Popovski, V., Caruana, J. A., Apostolopoulos, V. & McKenzie, I. F. C. (1998) *Cancer Immunol. Immunother.* **45,** 321–326.
29. Hart, G. W., Haltiwanger R. S., Holt, G. D. & Kelly, W. G. (1989) *Annu. Rev. Biochem.* **58,** 841–874.
30. Kihlberg, J. & Elofsson, M. (1997) *Curr. Med. Chem.* **4,** 85–116.
31. Vlad, A. M., Muller, S., Cudic, M., Paulsen, H., Otvos, L., Hanisch, F. G. & Finn, O. J. (2002) *J. Exp. Med.* **196,** 1435–1446.
32. Jensen, T., Galli-Stampino, L., Mouritsen, S., Frishce, K., Meldal, S. & Werdelin, O. (1999) *Eur. J. Immunol.* **26,** 1342–1349.
33. Jensen, T., Hansen, P., Galli-Stampino, L., Mouritsen, S., Frishce, K., Meinjohanns, E., Meldal, M. & Werdelin, O. (1999) *J. Immunol.* **158,** 3769–3778.
34. Kjellen, P., Brunsberg, U., Broddefalk, J., Hansen, B., Vestberg, M., Ivarsson, I., Engstrom, A., Svejgaard, A., Kihlberg, J., Fugger, L., *et al.* (1998) *Eur. J. Immunol.* **28,** 755–767.
35. Backlund, J., Carlsen, S., Hoger, T., Holm, B., Fugger, L., Kihlberg, J., Burkhardt, H. & Holmdahl, R. (2002) *Proc. Natl. Acad. Sci. USA* **99,** 9960–9965.
36. Dudler, T., Altmann, F., Carballido, J. M. & Blaser, K. (1995) *Eur. J. Immunol.* **25,** 538–542.
37. Harding, C. V., Kihlberg, J., Elofsson, M., Magnusson, G. & Unanue, E. R. (1993) *J. Immunol.* **151,** 2419–2425.
38. Deck, B., Elofsson, M., Kihlberg, J. & Unanue, E. R. (1995) *J. Immunol.* **155,** 1074–1078.
39. Kastrup, I. B., Stevanovic, S., Arsequell, G., Zeuthen, J., Rammensee, H. G., Elliott, T. & Haurum, J. S. (2000) *Tissue Antigens* **56,** 129–135.
40. Tirosh, B., el-Shami, K., Vaisman, N., Carmon, L., Feldman, M., Fridkin, M. & Eisenbach, L. (1999) *Immunol. Lett.* **70,** 21–28.
41. Scardino, A., Gross, D. A., Alves, P., Schultze, J. L., Graff-Dubois, S., Faure, O., Tourdot, S., Lemonnier, F. A. & Kosmatopoulos, K. (2002) *J. Immunol.* **168,** 5900–5906.